CONTACT AND SURFACE EFFECTS IN THE ELECTRIC FIELD INITIATION OF EXPLOSIVES (U)

THADDEUS GORA, ~~PhD;~~ JAGADISH SHARMA, ~~PhD;~~ DONALD A. WIEGAND, ~~PhD;~~
WAYNE L. GARRETT, ~~PhD;~~ DAVID S. DOWNS, ~~PhD.~~
EXPLOSIVES DIVISION, FELTMAN RESEARCH LABORATORY
PICATINNY ARSENAL, DOVER, NEW JERSEY 07801

INTRODUCTION

A number of explosive azides, including lead azide, can be initiated by the application of sufficient voltage *via* conducting electrical contacts. This occurs for both single crystal (1-4) and pressed pellet (5,6) samples. The effect is normally referred to as electric field initiaton and we shall adopt that terminology here. The related problem of the sensitivity of azide compounds to static electric charging and electric discharge has also received considerable attention (7). These phenomena are relevant to safety in the storage and handling of munitions items (lead azide is the Army's prevalent primary explosive), and to novel initiation mechanisms for potential fuzing applications (1,2).

A great deal of work has been done to characterize field initiation effects in explosives ~~(3,5,6)~~ and to understand them on the basis of the fundamental electronic, decomposition and conductivity properties ~~(1,2)~~ of the materials. ~~But~~ it has been difficult to relate experiments using single crystals (easiest to reproduce and understand) to experiments on pressed pellets and powders. ~~Our recent results and analysis~~, reported here, indicate that contact and surface effects are central to understanding the electric field initiation of explosives and to relating the results of experiments performed under different conditions and on different sample forms.

A. Background

An experiment which measures the threshold voltage for electric

field initiation of an explosive is basically straightforward. A sample is placed between two electrical contacts and a voltage applied in some prescribed manner until initiation is observed. On the other hand the analysis of the experiment is not at all straightforward; the effects of several parameters (such as the dielectric and conductivity properties of the explosive, the nature of the electrical contact and the particular sample-electrode geometry) must be taken into account. Only by considering these parameters can the electric field intensity, in the sample, be determined as a function of position. As we will show, it is a detailed knowledge of the field distribution which leads to an understanding of electric field initiation.

Our previous experiments (1,2,3) on lead azide [$Pb(N_3)_2$] using gold contacts and a sandwich geometry showed the following: Single crystals initiate upon the application of a voltage corresponding to an average threshold electric field (voltage/sample thickness) of 3.5×10^4 V/cm. Gold forms a blocking (non-injecting) contact to $Pb(N_3)_2$ under the conditions of the experiments. The voltage drop across the sample is relatively uniform near threshold voltages, i.e., the bulk of the sample experiences an electric field near the average field. The pressed pellet threshold average field approximates the single crystal value. Simultaneous application of low-intensity band gap radiation decreases the single crystal (but not the pressed pellet) threshold average field by a factor of two; this was explained qualitatively in terms of free charge motion and a consequent field redistribution resulting in higher electric field at the metal-explosive surface. Finally, the conductivity of $Pb(N_3)_2$ is very low, $\sim 10^{-12}$ $(ohm\text{-}cm)^{-1}$, while photoconductivity is up to four orders of magnitude higher.

Russian experiments (6) on cupric azide [$Cu(N_3)_2$] and thallous azide [$T\ell N_3$] pressed pellets found that threshold field values depend on the electronic work function of the metal contacts. This was interpreted to be evidence for the injection of charge. Experiments by Leopold (5) on $Pb(N_3)_2$ pressed pellets showed that no initiation occurs, even at much higher fields, if either or both of the electrodes were separated from the sample by thin mylar sheets.

In the analysis of experiments the dielectric constant of lead azide was generally taken to be ~ 5, based on pressed pellet data (8). The stoichiometry and impurity content of the lead azide powders were not characterized.

B. Approach

Our theoretical aims were twofold: to understand and model the Russian field initiation experiments (6) (the proposed explanation

appears neither reasonable nor useful in understanding other field initiation experiments); and to form a quantitative basis for understanding internal field distributions in azide explosives. The average threshold field value (voltage/sample thickness) simply does not provide sufficient information for comparative purposes.

Three areas of experimental work were indicated by the theoretical results and preliminary analysis. Leopold's experiments (5) were extended to single crystals and pellets of $Pb(N_3)_2$ at higher fields, and the effects of simultaneous irradiation examined. $Pb(N_3)_2$ single crystal dielectric constants were measured as a function of crystallographic direction. And the gross surface properties of explosive azides were examined by x-ray photoelectron spectroscopy.

The individual results are described in the next Sections, and are assembled into a general picture in the DISCUSSION Section.

THEORETICAL RESULTS

A. Initiation by Carrier Emission from Schottky Barrier Contacts

Recent Russian work on the initiation of $Cu(N_3)_2$ and $T\ell N_3$ by the application of a voltage to metal electrodes contacting high-density pressed pellets (0.02 cm thick) has revealed that the threshold field E_t for initiation depends on the electrode material (6). Three metals were examined. In order of increasing work function, they were Zn, Cu and W. With $Cu(N_3)_2$, it was found that E_t increases with increasing work function of the anode metal; and with $T\ell N_3$, that E_t decreases with increasing work function of the cathode metal (there is also a weaker dependence on anode metal). E_t values (using applied voltage/ sample thickness) corresponding to 50% initiation probability fell between $1.1\text{-}6.8 \times 10^4$ V/cm, with changes of 10-80% when the contact metals were varied.

This effect was associated with hole injection into the valence band in the case of $Cu(N_3)_2$, and with double injection into the valence and conduction bands in the case of $T\ell N_3$, in both cases followed by impact ionization (6). However, it is difficult to understand how the work function can play any significant role in a model based on current injection, for then (with the ohmic contacts that injection explicitly requires) current limitation is a bulk or volume phenomenon; and the electrodes should play no part other than to provide current carriers as the volume field conditions demand (9). In a later publication (10) the Russian group also qualitatively attributes the effect to the emission of carriers into the bulk at a Schottky-type barrier

contact (11) but offers no quantitative accounting of the electrode material-dependent initiation data (6). Such an accounting, together with a discussion of the limitations of the emission model, is provided by our theoretical model (12).

Considering $Cu(N_3)_2$ first, we demonstrate that an increase of E_t with anode metal work function is consistent with a model based on the emission of holes into the valence band at a Schottky barrier contact. The metal-$Cu(N_3)_2$ contact is viewed as that between a metal and a p-type semiconductor, as shown in Figure 1. Our detailed analysis

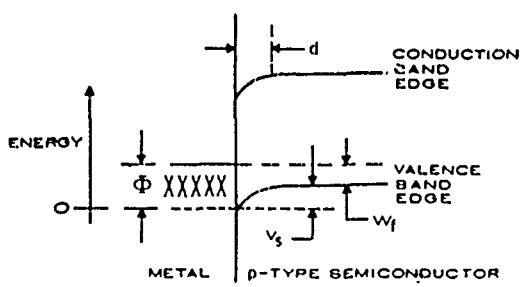

Figure 1. Energy band diagram for a p-type semiconductor-metal Schottky barrier contact with thickness d, barrier height Φ, surface potential V_s and Fermi energy W_f.

shows that when a back-bias voltage is applied to a Schottky barrier contact, the nonequilibrium electric field E_s at the interface in the presence of an applied voltage V is

$$E_s = A\,[V - W_m + \Gamma]^{1/2}; \qquad (1)$$

where A and Γ are related to material properties of the semiconductor only, and W_m is the metal work function. This shows that there can be a trade-off between W_m and a threshold applied voltage V_t (equivalent to an average applied electric field when scaled by the sample thickness) if initiation is associated with a critical interface field $E_{s,crit}$. The observation with $Cu(N_3)_2$ can then be understood qualitatively, for as the electrode work function increases V_t must also increase to have the right-hand side of Eq. 1 remain equal to a given constant $E_{s,\,crit}$ value.

For semi-quantitative agreement, V_t must be comparable to (or smaller than) $\Gamma - W_m$. In the Russian experiments V_t was approximately 400 volts, much larger than reasonable values for Γ (a few volts at most). Thus it would appear that our model does not apply. However, the samples were pressed pellets comprising individual powder grains that are most likely separated by potential barriers (13). In that event, the voltage drop across each grain, including those in contact with the electrodes, is V/n where n is the number of grains in the specimen thickness; and

further, the potential drop within each grain is predominantly across the surface barriers. Thus, if the grain diameter is about a micron (10^{-4} cm), n ≈ 200 and V_t is about 2 volts. Then V_t and Γ are of the same order and the model becomes plausible. Using reasonable values for semiconductor material properties and letting $V_t = \Gamma = 2$ volts yields (from Equation (1)) $E_{s,crit} = 2.2 \times 10^5$ volts/cm, a plausible value. Fields of 10^5 -10^6 volts/cm frequently cause destructive breakdown in other materials owing to carrier emission into the bulk.

Similar analysis shows the plausibility of viewing the metal-$T\ell N_3$ contact as that between a metal and an n-type semiconductor, with initiation associated with electron emission from the contact into the conduction band at a threshold $E_{s,crit}$.

B. Interface Electric Field Distributions in a Sandwich Geometry

The one-dimensional sample-electrode configuration considered is shown in Figure 2. The sample is a slab with parallel sides and thickness d, located symmetrically a distance $\ell/2$ away from two parallel capacitively coupled electrodes (electrode spacing is L). The static dielectric of the sample is ε, and that of the spacing material ε' (ε_o for free space). Complete field distributions were determined for three assumptions as to the nature of the specimen: perfect insulator, intrinsic semiconductor, and extrinsic semiconductor (uniform photo-excitation can be included in the last two cases) (14). For all non-uniform fields the maximum field value in the sample occurs at the surface, and so results for only the surface field are presented.

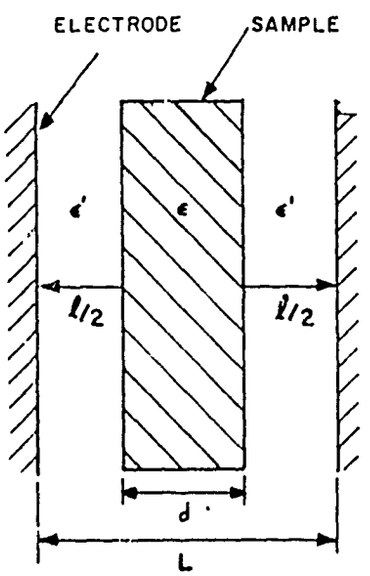

Figure 2. Sample of thickness d and dielectric constant ε between two electrodes separated by the distance L. The spacing material has the dielectric constant ε'.

In the perfect dielectic case, the field is uniform throughout the sample and so is equal to the surface field E_s, which is simply

$$E_s = \frac{V}{\kappa_r \ell + d} , \tag{2}$$

where $\kappa_r = \varepsilon/\varepsilon'$, the dielectric constant of the sample relative to that of the spacing medium. Equation (2) implies the following: For the case where the sample is directly contacted (ℓ=0), $E_s = V/L$. If the sample is thin ($d \ll L$), $E_s = V/\kappa_r L$. For given ℓ and d, increasing κ_r leads to a decreasing E_s.

In the intrinsic semiconductor case, mobile carriers of both signs accumulate on the surfaces and screen out the applied field. It is assumed that overall charge neutrality is maintained, and that no immobile free charge is present. If the uniform free charge density is ρ and the surface free charge per unit area σ is induced upon application of a voltage, $\sigma = \rho d$ up to the limit $\sigma_{max} = \varepsilon' V/\ell$ (in which case the field is totally screened from the sample). Then

$$E_s = \frac{V - \sigma\ell/\varepsilon'}{\kappa_r \ell + d} . \tag{3}$$

It is clear from Equation (3) that the presence of a uniform mobile free charge distribution can only lower the value of E_s from its perfect dielectric value (for constant V). This conclusion holds equally well for uniformly generated photo-carriers if both carrier types are mobile. The presence of free carriers of both types has the <u>effect</u> of changing the relative dielectric constant of Equation (2) by

$$\kappa_r \rightarrow \frac{\kappa_r V + \sigma d/\varepsilon'}{V - \sigma\ell/\varepsilon'} . \tag{4}$$

The extrinsic semiconductor case assumes that only one carrier type is mobile, and the compensating volume charge is present in the form of immobile charged impurities or trapped carriers. The analysis and results are more complicated, as two separate cases must be considered: complete sweep-out and partial sweep-out (of the mobile charge). In the former, the volume charge density ρ is insufficient to provide complete screening of the applied field anywhere in the sample. In the latter, a portion of the sample is completely screened. The complete sweep-out case occurs when ρ is less than a critical charge density ρ_{cr} (which depends on the voltage), and the partial sweep-out case when ρ exceeds ρ_{cr}, where

$$\rho_{cr} = \frac{2\,\varepsilon V}{d\,(2\kappa_r \ell + d)} . \tag{5}$$

The field at the surface is then

$$E_s = \frac{V + \rho d^2/2\varepsilon}{\kappa_r \ell + d} \quad \text{for } \rho<\rho_{cr} , \tag{6}$$

$$\text{and} \quad E_s = \frac{\rho \ell}{\varepsilon'} \{[1 + \frac{2\varepsilon' V}{\kappa_r \rho \ell^2}]^{1/2} - 1\} \text{ for } \rho>\rho_{cr} .$$

Both expressions in Equation (6) lead to larger values of E_s than do either of Equations (2) and (3). E_s increases monotonically with ρ, and its maximum change can be seen to be

$$\frac{E_s(\rho\to\infty)}{E_s(\rho=o)} = \frac{\kappa_r + d/\ell}{\kappa_r} \tag{7}$$

(note that this ratio approaches infinity as ℓ approaches zero).

Equations (2), (3) and (6) will be used in the following Sections to aid in the interpretation of experiments.

EXPERIMENTAL RESULTS

A. Threshold Initiation Fields in $Pb(N_3)_2$

All experiments were performed in the sandwich geometry of Figure 2. Prior results with direct explosive-metal contact were summarized above, and only the non-contacted experiments ($\ell \neq 0$ in Figure 2) are discussed here. The importance of using single crystal as well as pressed pellet samples is evident from the fact that the Schottky barrier model presented earlier explicitly requires the presence of intergrain barriers (for semiquantitative agreement with the Russian experiments). In the analysis of experiments with single crystals, only the barriers at the azide metal contacts are considered.

Samples were mounted between mylar insulators in a vacuum chamber at 2×10^{-5} torr. (The high voltage experiments reported by Leopold (5) were performed with the samples immersed in oil). Care was taken to avoid discharges from the high voltage points of the sample holder to ground. The voltage was increased in steps of 500 volts to a maximum of 5 kV, and was held constant for 30 sec at each step.

The expression appropriate to calculating the average electric field in the sample $\bar{E}$ is Equation (2), which is also the expression for the surface field if the field is uniform throughout the sample. Lead

azide's dielectric constant ($\varepsilon/\varepsilon_o$) was taken to be 5 for the values quoted in this Section.

No initiation occurred in the pressed pellet samples ($\sim$3.5 gm/cm^3 density, 1-3 x 10^{-2} cm thick), using the insulated electrodes, up to the highest $\bar{E}$ - values applied, 1.4x10^5 V/cm. This corresponds to the upper limit (5 kV) of the power supply for the sample dimensions used. It is a factor of four greater than the $\bar{E}$ - values that lead to initiation in contacted samples (1-3), and a factor of two greater than the highest $\bar{E}$ - value reported by Leopold (5). The same result (no initiation) held for single crystal samples (grown by the method of Garrett (15), and cut and polished to provide parallel flat surfaces), with the highest $\bar{E}$ - value attained being 1.02 x 10^5 V/cm. The highest $\bar{E}$ - values were maintained on the sample for about a half-hour. Some samples were subjected to combinations of 400.0 nm irradiation (strongly absorbed by $Pb(N_3)_2$) and a strong field, for both polarities, again with no initiation.

The results lead us to conclude that electrode interface effects dominate the field initiation of $Pb(N_3)_2$ single crystals and pressed pellets, with or without simultaneous low-level, strongly absorbed radiation, when the samples are directly contacted with the electrodes. Samples not directly contacted can sustain rather higher fields without initiation. It will be clear from the results below that only relative values of $\bar{E}$ are reliable from these experiments; they were performed without determining crystallographic orientation, and the dielectric constant will be seen to be strongly anisotropic.

B. Dielectric Constant Measurements on $Pb(N_3)_2$

Measurements were performed using both the GR-1615-A and GR-716-C capicitance bridges. The technique, and expressions used to deduce dielectric constants, are described elsewhere (16). The single crystal samples were grown by the method of Garrett (15), crystallographically oriented, and cut and polished into plates ($\sim$0.05 cm thick, and 0.1 cm^2 surface area).

The dielectric constants ($\varepsilon/\varepsilon_o$), measured along the unit cell axes, were found to be highly anisotropic: κ<100> = 17; κ<010> = 120; and κ<001> = 40. The experimental inaccuracy was $\pm$ 10%, and is a consequence of the difficulty of measuring the small evaporated electrode surface areas, the lack of perfectly parallel sample surfaces, and unaccounted edge capacitances. The values are frequency-independent at room temperature over the range 10^2 to 10^6 Hz. At a fixed frequency of 10^3 Hz, the dielectric constant varies slightly with temperature

(it has a positive slope), changing by 2% over the temperature range -100°C to + 100°C. The dissipation factor is small for each orientation ($<10^{-3}$), indicating negligible loss over the frequency range investigated.

The dielectric constant of $Pb(N_3)_2$ is thus both highly anisotropic and large compared to most other materials. The value determined for pressed pellets depends on the density and is lower than the lowest crystalline value because of averages over direction and voids. In any case, it is clear that the threshold initiation field experiments discussed earlier have to be done on oriented crystals in order to use Equation (12) to obtain reliable absolute values of $\bar{E}$; and that true average threshold field values for crystals are lower than those quoted earlier and in the literature.

C. Elemental Surface Composition Studies of Explosive Azides

The x-ray photoelectron spectroscopy (XPS) technique, and its application to the study of explosives, were described at a previous Army Science Conference (17). The technique determines the binding energies of electronic states by measuring the kinetic energies of x-ray-induced photoelectrons (using a monochromatic x-ray source). This allows elemental analysis, and yields information on the chemical states of observed elements. The signal from the first few surface layers makes the dominant contribution to the total XPS signal.

The XPS spectra were obtained with a Varian IEE-15 Spectrometer. The samples were either mounted as powders on Scotch Tape, sprayed onto a gold substrate from a methanol solution, or prepared by exposing the metal to HN_3 vapor. The powdered samples of alkali halides, alkali azides, thallous azide, and laboratory grade lead azide were freshly ground before mounting and insertion into the instrument. Silver azide, copper azide and commercial grade $Pb(N_3)_2$ were not ground. Light-sensitive samples were handled in weak sodium light. Details of the methods and approximations used to analyze the results are available elsewhere (18).

All samples showed significant surface contamination. Carbon is generally the dominant element detected, the amount being greater by a factor of three to ten over the constituents of the sample (taking relative cross-sections into account). The position of the C $1s_{1/2}$ peak indicates that the carbon is present in hydrocarbon form. Less oxygen contaminant is detected, but the amount is comparable to that of the host cation.

The degree of surface stoichiometry was examined by comparing intensity ratios of the sample's constituent elements (again taking relative cross sections into account). The results indicate that the

surface layers sampled were approximately stoichiometric for the following compounds (examined as a basis for comparison): NaCℓ, KBr, AgCℓ, TℓCℓ, KN_3 and RbN_3. In contrast, surface layers of the explosive azides $Pb(N_3)_2$, AgN_3, $T\ell N_3$, and $Cu(N_3)_2$ were generally deficient in azide content. In the cases of AgN_3, $T\ell N_3$, and $Pb(N_3)_2$, the degree of surface stoichiometry depends on the chemical preparation of the sample and also on its history. Freshly prepared samples of AgN_3 gave stoichiometric ratios between 0.6 and 0.9 (ratio of anion to cation concentration, normalized to unity for correct stoichiometry). Samples 2-3 years old gave values ranging from 0.2 to 0.4. When an old sample was exposed to aqueous vapors of HN_3 overnight, the stoichiometric ratio improved somewhat, but not to unity.

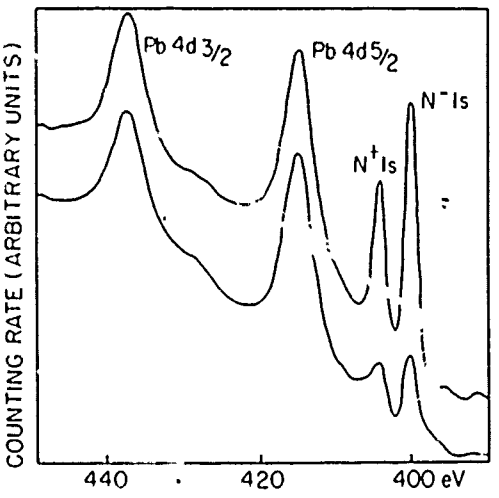

Figure 3. XPS spectra of $Pb(N_3)_2$, in a binding energy range having both Pb and N signals, for unirradiated (upper) and photo-decomposed (lower) samples.

The highest ratio (0.73) obtained for $Pb(N_3)_2$ was on samples freshly prepared and exposed to HN_3 vapor. The value for the upper curve of Figure 3 is 0.68. Samples which had been kept in the laboratory for a few months in the dark, and not freshly ground, gave values of $\sim$ 0.44. Commercial grade $Pb(N_3)_2$ had stoichiometric ratios ranging from 0.22 to 0.38. Samples subjected to sub-initiation level shocks showed an increase in the ratio. This is probably due to particle break-up and consequent exposure of fresh surfaces, assuming that the bulk of the material has a higher stoichiometry than the old surfaces.

Thallous azide exhibited behavior similar to that of lead azide. Aged samples showed a lack of stoichiometry on the surface, which could be increased to a value of unity by exposure to HN_3 vapors overnight.

All of the explosive azides investigated decompose when irradiated. This is illustrated in the lower curve of Figure 3, where the ratio of azide nitrogen to lead was considerably reduced by irradiation. In many samples of $Pb(N_3)_2$ and $T\ell N_3$, all nitrogen can be removed from the sample surface layers by irradiation. Irradiation of silver and copper azides removes all azide nitrogen signal, and the results suggest the formation of stable nitrides. In normal handling, azides are exposed to room light (irradiation). Thus non-stoichiometry and the presence of other compounds at the surfaces which will influence electrical contact properties can be expected.

It appears that surface layers on lead azide form a protective coating, preventing further decomposition with aging (otherwise, a twenty-year-old sample would not give any azide signal). This is consistent with the fact that shock waves improve stoichiometry due to cracking and exposing of new surfaces. In addition, twenty-year-old samples can be detonated, indicating appreciable azide content in the bulk although the surface stoichiometry is poor.

DISCUSSION

Our results have been discussed individually in earlier Sections. A more general discussion is performed here relating them to each other and to prior results. The most important conclusion is that contact and surface effects dominate the electric field initiation properties of explosive azides, and that this can explain apparent discrepancies when comparing experiments performed under dissimilar conditions. The detailed mechanisms involved are not fully understood, but the nature of the crucial experiments and calculations are now clear.

The Russian field initiation experiments (6) provided an important clue to the role of interface contacts. Our theoretical model shows that the experiments using non-ohmic metal contacts can be explained if initiation is the result of a critical threshold field $E_{s,crit}$ at the metal-explosive interface. A different value of $E_{s,crit}$ would then be associated with each explosive azide, and be independent of the nature of the non-ohmic metal contact (so long as a contact is available); its magnitude is of the order of 10^5 V/cm in $Cu(N_3)_2$ and $T\ell N_3$. Recall that our model cannot explain these experimental results without explicitly taking the pressed pellet nature of the samples into account. The field initiation experiments on contacted $Pb(N_3)_2$ samples appear also to require a critical interface field.

These conclusions point to an initiation model involving carrier emission from a barrier contact. Two alternative mechanisms are suggested for this emission model based on field breakdown mechanisms in the literature. Both rely on high local internal fields to generate

hot electrons, which can then cause impact ionization. The first, due to O'Dwyer (19), assumes that the impact ionizacion leads to avalanche multiplication with eventual breakdown at the exit electrode, where most of the energy of impact-generated carriers is dissipated. The second mechanism, due to DiStefano and Shatzkes (20), suggests that impact ionization generates a space charge in the volume of the sample which concentrates the internal field at the emitting electrode; this in turn produces an increase in the emission current, with eventual catastrophic power dissipation at the entrance electrode. The choice between the two mechanisms (for a given explosive azide) can thus be made on the basis of experiments that determine whether initiation occurs near the entrance or exit electrode.

The experiments of Leopold (5), and their extensions reported here, showed that no initiation occurs without direct metallic contact up to the limits of the experimental apparatus. This is consistent with the emission model just presented. Values for the interface fields E_s attained can be calculated from Equation (2) by using the appropriate dielectric constant κ_r. Lead azide's dielectric constant was found to be large and highly anisotropic. Thus single crystal experiments on oriented samples must be performed to establish reliable values of the highest E_s attained in the samples; and other experiments testing at what value of E_s initiation occurs, without direct contact, would be valuable.

Our previous model for the photo-electronic initiaton effect (decrease in average threshold field for initiation when strongly absorbed light is applied simultaneously) involved a redistribution of the electric field as a consequence of the illumination. The analysis of the field initiation experiments provides a more quantitative basis for this model. We assume that $Pb(N_3)_2$ is highly insulating (a perfect dielectric), and acts as an extrinsic semiconductor upon irradiation. Equations (6) and (7) then describe the increase in E_s that can result from a uniformly absorbed radiation pulse. The analysis must be expanded to include non-uniformly absorbed irradiation (which is straightforward), and also the direct (ℓ=0) metallic contact situation (as in the Schottky barrier analysis).

Finally, our surface studies of explosive azides give the first unambiguous picture of the topmost several layers of these materials. The presence of contamination and absence of stoichiometry in even laboratory quality sample surfaces apparently results from the highly reactive nature of the surfaces. This may explain why attempts to find injecting contacts have not been successful, and also how to overcome this problem. The relation between prior treatment of azide surfaces and the sensitivity of explosive azide powders bears closer scrutiny.

CONCLUSIONS

An integrated experimental and theoretical program to understand the field initiation properties of explosive azides has resulted in an important broad conclusion. Contact and surface effects dominate the electric field initiation properties of these materials. This realization has been successfully used to relate the results of experiments performed under different conditions on different sample forms.

The results and understanding are directly relevant to a number of novel fuzing device applications (e.g., fuzes that require more than one stimulus to fire), and to safety against electrical and electrostatic hazards in the storage and handling of munitions.

ACKNOWLEDGEMENTS

We are most grateful to Professor Peter Mark of Princeton University for his considerable contributions to all phases of this work, to Dr. Harry D. Fair, Jr. for his direction and comments, and to Dr. R. F. Walker for his support.

REFERENCES

1. H.D.Fair, Jr, D.S. Downs, A.C. Forsyth, W. Garrett, M. Blais, T. Gora and F.E. Williams, Picatinny Arsenal Technical Report 4607, December 1973.
2. D.S. Downs, W. Garrett, D.A. Wiegand, T. Gora, M. Blais, A.C. Forsyth and H.D. Fair, Jr., Picatinny Arsenal Technical Report 4711, September 1974.
3. D.S. Downs, T. Gora, M. Blais and W.L. Garrett, Picatinny Arsenal Technical Report 4874, November 1975.
4. F.P. Bowden and A.C. McLaren, Proc. Roy. Soc. A246, 197 (1958).
5. H.S. Leopold, Naval Ordnance Laboratory Technical Report 73-125 (1973).
6. Y.A. Zakharov and Y.N. Sukhushin, Izv. Tomsk Politeckh. Inst. 251, 213 (1970).
7. M.S. Kirshenbaum, Picatinny Arsenal Technical Report 4559 (1973).
8. J.E. Schiviner, Sandia Laboratories, Report No. 73-5001 (1973).
9. M.A. Lampert and P. Mark, "Current Injection in Solids", Chap. 1, Academic Press, New York (1970).
10. Y.N. Sukhushin, Y.A. Zakharov, and F.I. Ivanov, Khim. Vys. Energiy 7, 261 (1973).
11. S.M. Sze, "Physics of Semiconductor Devices", Chap. 8, John Wiley and Sons, New York (1969).
12. P. Mark and T. Gora, J. Solid State Chem. 15, 79 (1975).
13. R.H. Bube, J. Appl. Phys. 31, 2239 (1960); P. Mark and B.W. Lee, J. Phys. Chem. Solids 35, 865 (1974).
14. T. Gora and P. Mark (unpublished calculations).

15. W.L. Garrett, Mat. Res. Bull. 7, 949 (1972).
16. W.L. Garrett, Mat. Res. Bull. (to be submitted).
17. J. Sharma, T. Gora, S. Bulusu and D.A. Wiegand, Proceedings of the Army Science Conference, West Point, N.Y. (1974).
18. P. DiBona, D.A. Wiegand and J. Sharma, J. Vac. Sci. Tech. (in press).
19. J.J. O'Dwyer, J. Appl. Phys. 40, 3887 (1969).
20. T.H. DiStefano and M. Shatzkes, Appl. Phys. Lett. 25, 685 (1974); J. Vac. Sci. Tech. 12, 493 (1975).